Research Article | Vol. 26, No. 5 | 5 Mar 2018 | OPTICS EXPRESS 5531
Optics EXPRESS

Comparison of phase quadrature squeezed states generated from degenerate optical parametric amplifiers using PPKTP and PPLN

ZHENJU WAN,[1] JINXIA FENG,[1,2] YUANJI LI,[1,2] AND KUANSHOU ZHANG[1,2,*]

[1]*State Key Laboratory of Quantum Optics and Quantum Optics Devices, Institute of Opto-Electronics, Shanxi University, Taiyuan 030006, China*
[2]*Collaborative Innovation Center of Extreme Optics, Shanxi University, Taiyuan 030006, China*
**kuanshou@sxu.edu.cn*

Abstract: Phase quadrature squeezed states at 1550 nm generated from degenerate optical parametric amplifiers (DOPAs) using periodically poled $KTiOPO_4$ (PPKTP) and periodically poled lithium niobate (PPLN) are compared. A squeezing of 6.8 dB was produced from the DOPA using PPKTP with the phase matching temperature of 34.5 °C. By contrast, a measured squeezing of 4.9 dB was generated using PPLN with the phase matching temperature of 135.2 °C. The degradation of squeezing using a nonlinear crystal with a high phase matching temperature is explained by a theoretical model of DOPAs including the extra phase noise caused by the guided acoustic wave Brillouin scattering within the nonlinear crystal.

OCIS codes: (270.0270) Quantum optics; (270.6570) Squeezed states; (270.2500) Fluctuations, relaxations, and noise.

References and links

1. S. L. Braunstein and P. van Loock, "Quantum information with continuous variables," Rev. Mod. Phys. **77**(2), 513–577 (2005).
2. U. L. Andersen, T. Gehring, C. Marquardt, and G. Leuchs, "30 years of squeezed light generation," Phys. Scr. **91**(5), 053001 (2016).
3. A. Furusawa, J. L. Sorensen, S. L. Braunstein, C. A. Fuchs, H. J. Kimble, and E. S. Polzik, "Unconditional quantum teleportation," Science **282**(5389), 706–709 (1998).
4. N. C. Menicucci, P. van Loock, M. Gu, C. Weedbrook, T. C. Ralph, and M. A. Nielsen, "Universal quantum computation with continuous-variable cluster states," Phys. Rev. Lett. **97**(11), 110501 (2006).
5. T. Aoki, G. Takahashi, T. Kajiya, J. Yoshikawa, S. L. Braunstein, P. van Loock, and A. Furusawa, "Quantum error correction beyond qubits," Nat. Phys. **5**(8), 541–546 (2009).
6. A. A. Berni, T. Gehring, B. M. Nielsen, V. Händchen, M. G. A. Paris, and U. L. Andersen, "Ab initio quantum-enhanced optical phase estimation using real-time feedback control," Nat. Photonics **9**(9), 577–581 (2015).
7. The LIGO Scientific Collaboration, "gravitational wave observatory operating beyond the quantum shot-noise limit," Nat. Phys. **7**(12), 962–965 (2011).
8. T. L. S. Collaboration, "Enhanced sensitivity of the LIGO gravitational wave detector by using squeezed states of light," Nat. Photonics **7**(8), 613–619 (2013).
9. H. Yonezawa, D. Nakane, T. A. Wheatley, K. Iwasawa, S. Takeda, H. Arao, K. Ohki, K. Tsumura, D. W. Berry, T. C. Ralph, H. M. Wiseman, E. H. Huntington, and A. Furusawa, "Quantum-enhanced optical-phase tracking," Science **337**(6101), 1514–1517 (2012).
10. N. Treps, U. Andersen, B. Buchler, P. K. Lam, A. Maître, H.-A. Bachor, and C. Fabre, "Surpassing the standard quantum limit for optical imaging using nonclassical multimode light," Phys. Rev. Lett. **88**(20), 203601 (2002).
11. J. X. Feng, X. T. Tian, Y. M. Li, and K. S. Zhang, "Generation of a squeezing vacuum at a telecommunication wavelength with periodically poled $LiNbO_3$," Appl. Phys. Lett. **92**(22), 221102 (2008).
12. M. Mehmet, S. Steinlechner, T. Eberle, H. Vahlbruch, A. Thüring, K. Danzmann, and R. Schnabel, "Observation of cw squeezed light at 1550 nm," Opt. Lett. **34**(7), 1060–1062 (2009).
13. M. Mehmet, S. Ast, T. Eberle, S. Steinlechner, H. Vahlbruch, and R. Schnabel, "Squeezed light at 1550 nm with a quantum noise reduction of 12.3 dB," Opt. Express **19**(25), 25763–25772 (2011).
14. Q. C. Sun, Y. L. Mao, Y. F. Jiang, Q. Zhao, S. J. Chen, W. Zhang, W. J. Zhang, X. Jiang, T. Y. Chen, L. X. You, L. Li, Y. D. Huang, X. F. Chen, Z. Wang, X. Ma, Q. Zhang, and J. W. Pan, "Entanglement swapping with independent sources over an optical-fiber network," Phys. Rev. A **95**(3), 032306 (2017).
15. J. Feng, Z. Wan, Y. Li, and K. Zhang, "Distribution of continuous variable quantum entanglement at a telecommunication wavelength over 20 km of optical fiber," Opt. Lett. **42**(17), 3399–3402 (2017).

#312486 https://doi.org/10.1364/OE.26.005531
Journal © 2018 Received 2 Nov 2017; revised 24 Jan 2018; accepted 19 Feb 2018; published 23 Feb 2018

Optics EXPRESS

16. L. A. Wu, H. J. Kimble, J. L. Hall, and H. Wu, "Generation of squeezed states by parametric down conversion," Phys. Rev. Lett. **57**(20), 2520–2523 (1986).
17. A. Heidmann, R. J. Horowicz, S. Reynaud, E. Giacobino, C. Fabre, and G. Camy, "Observation of quantum noise reduction on twin laser beams," Phys. Rev. Lett. **59**(22), 2555–2557 (1987).
18. E. S. Polzik, J. Carri, and H. J. Kimble, "Spectroscopy with squeezed light," Phys. Rev. Lett. **68**(20), 3020–3023 (1992).
19. S. Suzuki, H. Yonezawa, F. Kannari, M. Sasaki, and A. Furusawa, "7dB quadrature squeezing at 860nm with periodically poled $KTiOPO_4$," Appl. Phys. Lett. **89**(6), 061116 (2006).
20. Y. Takeno, M. Yukawa, H. Yonezawa, and A. Furusawa, "Observation of -9 dB quadrature squeezing with improvement of phase stability in homodyne measurement," Opt. Express **15**(7), 4321–4327 (2007).
21. M. Lassen, M. Sabuncu, P. Buchhave, and U. L. Andersen, "Generation of polarization squeezing with periodically poled KTP at 1064 nm," Opt. Express **15**(8), 5077–5082 (2007).
22. M. Lassen, M. Sabuncu, A. Huck, J. Niset, G. Leuchs, N. J. Cerf, and U. L. Andersen, "Quantum optical coherence can survive photon losses: a continuous-variable quantum erasure correcting code," Nat. Photonics **4**(10), 700–705 (2010).
23. H. Vahlbruch, M. Mehmet, K. Danzmann, and R. Schnabel, "Detection of 15 dB squeezed states of light and their application for the absolute calibration of photoelectric quantum efficiency," Phys. Rev. Lett. **117**(11), 110801 (2016).
24. F. Kaiser, B. Fedrici, A. Zavatta, V. D'auria, and S. Tanzilli, "A fully guided-wave squeezing experiment for fiber quantum network," Optica **3**(4), 362–364 (2016).
25. J. E. S. César, A. S. Coelho, K. N. Cassemiro, A. S. Villar, M. Lassen, P. Nussenzveig, and M. Martinelli, "Excess phase noise from thermal fluctuations in nonlinear optical crystals," Phys. Rev. A **79**(6), 063816 (2009).
26. D. Elser, U. L. Andersen, A. Korn, O. Glöckl, S. Lorenz, Ch. Marquardt, and G. Leuchs, "Reduction of guided acoustic wave Brillouin scattering in photonic crystal fibers," Phys. Rev. Lett. **97**(13), 133901 (2006).
27. M. J. Lawrence, R. L. Byer, M. M. Fejer, W. Bowen, P. K. Lam, and H.-A. Bachor, "Squeezed singly resonant second-harmonic generation in periodically poled lithium niobate," J. Opt. Soc. Am. B **19**(7), 1592–1598 (2002).
28. L. E. Myers, R. C. Eckardt, M. M. Fejer, R. L. Byer, W. R. Bosenberg, and J. W. Pierce, "Quasi-phase matched optical parametric oscillators on bulk periodically poled $LiNbO_3$," J. Opt. Soc. Am. B **12**(11), 2102–2116 (1995).
29. N. B. Grosse, S. Assad, M. Mehmet, R. Schnabel, T. Symul, and P. K. Lam, "Observation of entanglement between two light beams spanning an octave in optical frequency," Phys. Rev. Lett. **100**(24), 243601 (2008).
30. N. B. Grosse, "Harmonic entanglement & photon anti-bunching," (PhD thesis, the Australian national university, Australian, 2009). http://photonics.anu.edu.au/theses/Thesis%20ANU%20PhD%202009%20Grosse.pdf
31. M. Shirasaki and H. A. Haus, "Reduction of guided-acoustic-wave Brillouin scattering noise in a squeezer," Opt. Lett. **17**(17), 1225–1227 (1992).
32. H. Zhou, W. Yang, Z. Li, X. Li, and Y. Zheng, "A bootstrapped, low-noise, and high-gain photodetector for shot noise measurement," Rev. Sci. Instrum. **85**(1), 013111 (2014).
33. N. Lastzka, J. Steinlechner, S. Steinlechner, and R. Schnabel, "Measuring small absorptions by exploiting photothermal self-phase modulation," Appl. Opt. **49**(28), 5391–5398 (2010).

1. Introduction

Squeezed states are important resources for quantum information processing with continuous variables [1,2]. For example, squeezed states are used to realize quantum teleportation [3], quantum computing [4], quantum error correction coding [5], and phase estimation [6]. Meanwhile, squeezed states have great potential in high-precision quantum measurements such as gravitational waves detector [7,8], optical-phase tracking [9] and quantum imaging [10]. Generation of squeezed states at telecommunication wavelength of 1550 nm have been recently a very interesting issue due to the lowest optical power attenuation of light at this wavelength in standard telecommunication fibers [11–13]. The squeezed states at wavelength of 1550 nm in combination with existing fiber telecommunication networks offers the possibility to implement long-distance quantum communication [14,15].

Optical parametric oscillator (OPO) and amplifier (OPA) have been often used to generate squeezed states [16–18]. Using bulk nonlinear crystals, such as $MgO:LiNbO_3$ [16], $KTiOPO_4$ (KTP) [17] and $KNbO_3$ [18], the achievable squeezing degree leveled around 6 dB. Then periodically poled nonlinear crystals have been used in OPO and OPA, because their long interaction lengths and the largest nonlinear coefficients can be utilized. Thereby 7.2 dB and 9 dB squeezing have been achieved in 2006 and 2007 with a periodically poled KTP (PPKTP) crystal, respectively [19,20]. A polarization squeezing at 1064 nm was first generated and a quantum error correcting scheme was performed using PPKTP crystal [21,22]. So far, a maximum squeezing degree of 15 dB at 1064 nm using a semi-monolithic OPO cavity with a PPKTP crystal was reported [23]. At the telecommunication wavelength around 1550 nm, 2.4

Optics EXPRESS

dB squeezing vacuum was observed firstly utilizing a subthreshold OPO with a periodically poled lithium niobate (PPLN) crystal [11], 12.3 dB squeezing vacuum was obtained using a PPKTP crystal [13], and 1.83 dB single-mode squeezing was generated utilizing PPLN ridge waveguide [24]. Although a higher frequency conversion efficiency can be achieved using PPLN owing to its larger effective nonlinearity (d_{eff} ~19 pm/V), the largest squeezing degree of squeezed state was realized using PPKTP in spite that PPKTP offers moderate effective nonlinear coefficient (d_{eff} ~10 pm/V). It is well known that the phase matching temperature of PPLN is usually more than 100 °C in order to avoid photorefractive effects and optical damage, so the squeezing degree of squeezed state using PPLN is relative low can be attributed to there is extra phase noise in OPO or OPA. J. César *et al*. considered the source of extra phase noise observed in OPOs was the scattered light by thermal phonons inside a second-order nonlinear crystal [25], and D. Elser *et al.* explained the excess phase noise for light transmitting through the optical fiber by a guided acoustic wave Brillouin scattering (GAWBS) model [26].

In this paper, bright phase quadrature squeezed states at 1550 nm are generated from degenerate OPAs (DOPAs) using PPLN and PPKTP, respectively. The classical and quantum characteristics of DOPAs are observed experimentally and analysed theoretically. A theoretical model of DOPAs including the extra phase noise caused by the effect of GAWBS within the nonlinear crystal is used to explain the degradation of squeezing degree of generated squeezed state.

2. Theoretical description

2.1 Model

The DOPA device, which is pumped by harmonic wave (2ω) and injected by subharmonic wave (ω), is shown in Fig. 1. A type-I phase matched periodically poled crystal (PPXX, such as PPLN and PPKTP) is employed. $\chi^{(2)}$ is the second-order nonlinear coefficient of the PPXX crystal. The subharmonic wave resonates in the DOPA cavity and the harmonic wave double-passes through the crystal. $\alpha_{p,in}$ ($\alpha_{s,in}$) is the input mode operator of harmonic (subharmonic) wave, α_0 (α) is the harmonic (subharmonic) mode operator in the cavity, $\alpha_{p,out}$ ($\alpha_{s,out}$) is the output mode operator of harmonic (subharmonic) wave.

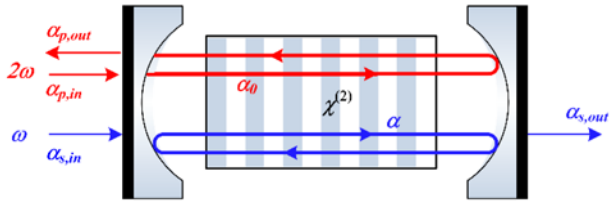

Fig. 1. Schematic of the degenerate optical parametric amplifier.

Assuming zero detuning of the cavity, the quantum Langevin equations of motion for the intracavity modes are as follows [27]

$$\begin{cases} \dot{\alpha}_0 = -\gamma_0\alpha_0 - \kappa/2\,\alpha^2 + \sqrt{2\gamma_{01}}\,\alpha_{p,in} + \sqrt{2\gamma_{0c}}\,C_{0,in} \\ \dot{\alpha} = -\gamma\alpha + \kappa\alpha_0\alpha^+ + \sqrt{2\gamma_1}\,\alpha_{s,in} + \sqrt{2\gamma_c}\,C_{1,in} \end{cases}, \tag{1}$$

where $\gamma = \gamma_1 + \gamma_c + \gamma_2$ is the total cavity photon loss rate of the subharmonic wave, $\gamma_0 = \gamma_{01} + \gamma_{0c} + \gamma_{02}$ is the total cavity photon loss rate of the harmonic wave. γ_1 (γ_{01}), γ_c (γ_{0c}), γ_2 (γ_{02}) are the photon loss rates due to the input coupler transmission, the internal cavity losses and the output coupler transmission of the subharmonic (harmonic) wave, respectively. The internal cavity losses include crystal absorption, surface scattering, and imperfections of mirrors,

Optics EXPRESS

which are taken into account by introducing a coupling to the vacuum mode $C_{1,in}$ ($C_{0,in}$) of zero mean for the subharmonic (harmonic) wave. κ is the nonlinear coupling coefficient.

The input-output relation of the subharmonic wave is given by

$$\alpha_{s,out} = \sqrt{2\gamma_2}\alpha. \tag{2}$$

The steady state solution of Eq. (1) can be written as

$$-\mu\alpha^3 + \left[2\sqrt{\mu}\alpha_{p,in} - \gamma\right]\alpha + \sqrt{2\gamma_1}\alpha_{s,in} = 0, \tag{3}$$

where μ is the two photon damping rate. The threshold of OPO is $\alpha_{th} = \gamma/\sqrt{2\mu}$ with vacuum subharmonic input ($\alpha_{s,in} = 0$). μ can be expressed as [28]:

$$\mu = \frac{\hbar\omega}{2\tau^2}\left(\frac{2}{\pi m}\right)^2 \frac{8\pi^2 d_{eff}^2}{n_1^2 n_2 \lambda^2 \varepsilon_0 c}\sin c^2\left(\frac{\Delta k \cdot L}{2}\right), \tag{4}$$

where L and d_{eff} are the length and effective nonlinear coefficient of the PPXX crystal, respectively; n_1 and n_2 are the indices of refraction of the PPXX crystal at optical frequency ω and 2ω, respectively; λ is the wavelength of subharmonic wave; ε_0 is the permittivity of free space and c is the speed of light. Δk is the wavevector mismatch between the subharmonic and harmonic waves in the PPXX crystal. m is the order of the phase matching of crystal. τ is the cavity round-trip time.

2.2 Quantum fluctuation

The quantum properties of the DOPA device can be derived using well-established techniques. We linearize the equations of motion (1) for small fluctuations $\delta\alpha_i$ around the mean field value $\bar{\alpha}_i$, where $\bar{\alpha}_i$ represents $\bar{\alpha}_{p,in}, \bar{\alpha}_{s,in}, \bar{\alpha}_0$ and $\bar{\alpha}$. The amplitude and phase quadratures can be defined by $X_i^+ = a_i + a_i^+$ and $X_i^- = -i\left(a_i - a_i^+\right)$. The fluctuation equations of motion for the subharmonic field in the cavity can be obtained as

$$\delta\dot{X}^{\pm} = -(\gamma + 2\mu\bar{\alpha}^2)\delta X^{\pm} \pm (\sqrt{2\mu}\bar{\alpha}_{p,in} - \mu\bar{\alpha}^2)\delta X^{\pm} + 2\sqrt{\mu}\bar{\alpha}\delta X_{p,in}^{\pm} + \sqrt{2\gamma_1}\delta X_{s,in}^{\pm} + \sqrt{2\gamma_{1c}}\delta X_{C,in}^{\pm}, \tag{5}$$

where $\delta X_{C,in}^{\pm}$ are the vacuum fluctuations.

The extra phase noise existed within the second-order nonlinear crystal will reduce the phase quadrature squeezing from the DOPA device. The extra phase noise can be attributed to the effect of GAWBS within the nonlinear crystal [29]. The acoustic elastic modes (AEMs) of the crystal are excited by the thermal energy of the crystal, and the standing pressure waves caused by AEMs modulate the phase of light throughout the crystal. So the fluctuation equation of motion for the phase quadrature can be rewritten as

$$\delta\dot{X}^{-} = -(\gamma + 2\mu\bar{\alpha}^2)\delta X^{-} - (\sqrt{2\mu}\bar{\alpha}_{p,in} - \mu\bar{\alpha}^2)\delta X^{-} + 2\sqrt{\mu}\bar{\alpha}\delta X_{p,in}^{-} + \sqrt{2\gamma_1}\delta X_{s,in}^{-} + \sqrt{2\gamma_{1c}}\delta X_{C,in}^{-} + \delta Q_G, \tag{6}$$

where δQ_G is the fluctuation of the extra phase noise induced by GAWBS.

Taking the Fourier transform of Eq. (6), the spectrum of the phase quadrature noise can be gotten as

$$\delta X^{-}(\Omega) = \frac{2\sqrt{\mu}\bar{\alpha}\delta X_{p,in}^{-}(\Omega) + \sqrt{2\gamma_1}\delta X_{s,in}^{-}(\Omega) + \sqrt{2\gamma_{1c}}\delta X_{C,in}^{-}(\Omega) + \delta Q_G(\Omega)}{\gamma + \mu\bar{\alpha}^2 + \sqrt{2\mu}\bar{\alpha}_{p,in} - i2\pi\Omega}, \tag{7}$$

Optics EXPRESS

where Ω is the analysis frequency in the unit of hertz.

Using input-output relation of Eq. (2), the phase quadrature fluctuation of the output subharmonic field can be deduced as

$$\delta X_{out}^{-}(\Omega)=\sqrt{2\gamma_2}\cdot\frac{2\sqrt{\mu\bar{\alpha}}\delta X_{p,in}^{-}(\Omega)+\sqrt{2\gamma_1}\delta X_{s,in}^{-}(\Omega)+\sqrt{2\gamma_{1c}}\delta X_{C,in}^{-}(\Omega)+\delta Q_G(\Omega)}{\gamma+\mu\bar{\alpha}^2+\sqrt{2\mu}\bar{\alpha}_{p,in}\text{-}i2\pi\Omega}. \quad (8)$$

Assuming that the fluctuations of pump and noise induced by extra losses are uncorrelated and with the variance of 1, the spectrum of the output variance can be obtained using Eq. (8),

$$Var(\delta X_{out}^{-})=1-4\xi\eta\zeta\frac{\sigma-\mu\bar{\alpha}^2/\gamma-V_{Q_G}}{(1+\mu\bar{\alpha}^2/\gamma+\sigma)^2+\Omega_c{}^2}, \quad (9)$$

where $\xi=\sqrt{\gamma_2/\gamma}$ is escape efficiency. η is the quantum efficiency of the photodiode and ζ is the homodyne efficiency, which should be considered during an actual detection. $\Omega_c=\Omega/\gamma$ is the normalized analysis frequency. The normalized pump power is defined as $\sigma=P_{pump}/P_{th}$. The variance of the extra phase noise induced by GAWBS can be written as [30]

$$V_{Q_G}=\sqrt{2\eta_G}\bar{\alpha}, \quad (10)$$

where $\eta_G=(\varphi/2)^2$ is the Brillouin scattering efficiency, and $\varphi=\frac{2\pi L}{\lambda}\Delta n$ is the phase shift caused by the change of the refractive index of nonlinear crystal (Δn). Δn is induced by AEM that is related to the nonlinear crystal temperature and the modulation frequency. GAWBS, even though occurring at modulation frequencies higher than 20 MHz, can constitute a significant thermal noise source to the generation of squeezed states at low-frequencies [31].

Figure 2 gives the calculated Brillouin scattering efficiency and relative extra phase noise induced by GAWBS as functions of temperature of PPXX crystal [Fig. 2(a)] and normalized pump power [Fig. 2(b)], respectively. The relative phase noise means the extra phase noise power induced by GAWBS within the nonlinear crystal relative to that when the temperature of nonlinear crystal is 0 °C. The solid curves (i) and (ii) in Fig. 2 correspond to the Brillouin scattering efficiencies of PPKTP and PPLN, respectively. The dashed curves (iii) and (iv) in Fig. 2 correspond to the relative extra phase noise induced by GAWBS inside PPKTP and PPLN, respectively. In our calculation, the length of the PPXX crystal is set as 10 mm. In Fig. 2(a), the normalized pump power $\sigma=0.7$ that is optimal to obtain maximum squeezing in our experiments. It can be seen, the Brillouin scattering efficiency increases with increasing PPXX temperature, and the Brillouin scattering efficiency of PPLN is obviously larger and increases faster than that of PPKTP. The results also indicate that the extra phase noise inside PPXX can be reduced by lowering the temperature of nonlinear crystals. In Fig. 2(b), the work temperatures of PPKTP and PPLN are set as 35 °C and 136 °C, respectively, which are optimal phase matching temperatures for DOPAs in our experiments. Clearly, the Brillouin scattering efficiency and the extra phase noise within PPLN are larger and increase faster than that of PPKTP. Consequently, the influence of extra phase noise induced by the effect of GAWBS on the squeezing generated using PPKTP is smaller than that using PPLN.

Optics EXPRESS

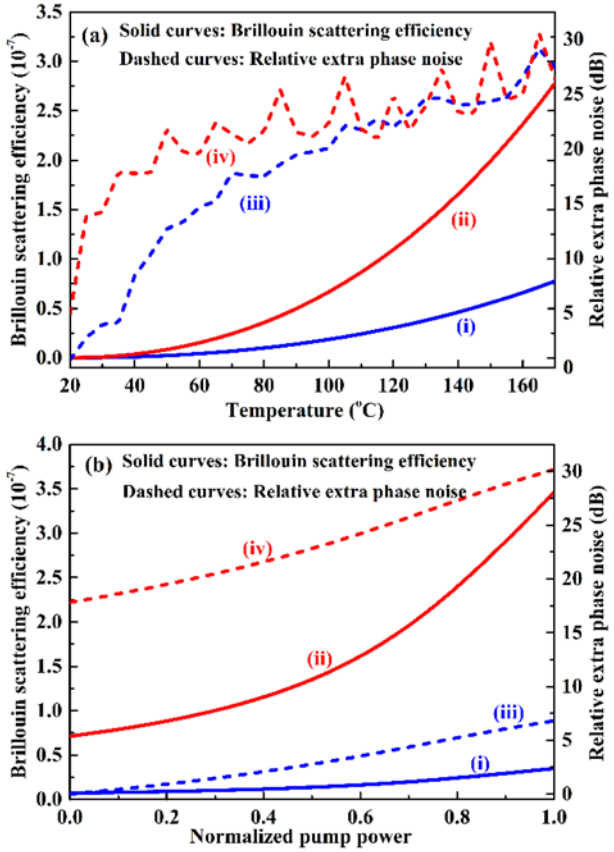

Fig. 2. Calculated Brillouin scattering efficiency and relative extra phase noise induced by the effect of GAWBS as functions of temperature of PPXX crystal (a) and normalized pump power (b). Solid curves (i) and (ii) correspond to the Brillouin scattering efficiency of PPKTP and PPLN, respectively. Dashed curves (iii) and (iv) correspond to the relative extra phase noise induced by the effect of GAWBS inside PPKTP and PPLN, respectively.

3. Experimental setup

The schematic of the experimental setup used to generate squeezing states is shown in Fig. 3. A commercial fiber laser (NP Photonic Inc.) provided an output power of 2.0 W with continuous-wave (CW) single-frequency operation at 1550 nm. An optical isolator (OI) was used to eliminate the back-reflection light. The laser beam was sent through a mode clear (MC1) with a finesse of 500 and linewidth of 600 kHz for preliminary filtering of the laser spatial mode and extra intensity noise. An electro-optical modulator (EOM) with a radio frequency of 65 MHz was employed to lock the MC1 cavity using the Pound-Drever-Hall (PDH) technique. The output from MC1 was split into two parts. The main portion was injected into an external enhanced second harmonic generation (SHG) cavity to obtain a high-power, low-noise CW laser with a wavelength of 775 nm that acted as the pump of the DOPA. The residual portion was used as the injected signal of the DOPA and the local oscillator (LO) of the detection system. The external enhanced SHG cavity was composed of a linear cavity and a PPLN crystal. A 1 W single-frequency laser at 775 nm was obtained with the frequency doubling efficiency of 85%. MC2, with a linewidth of 700 kHz, was used to reduce the excess intensity noises of the pump of the DOPA. MC2 was also locked using the PDH technique with a radio frequency of 82 MHz. The power transmittances of the two MCs were approximately 80%. Using the MCs, the intensity noises of the pump and injected signal of the DOPA reached the shot noise level (SNL) for analysis frequencies higher than 4 MHz.

Optics EXPRESS

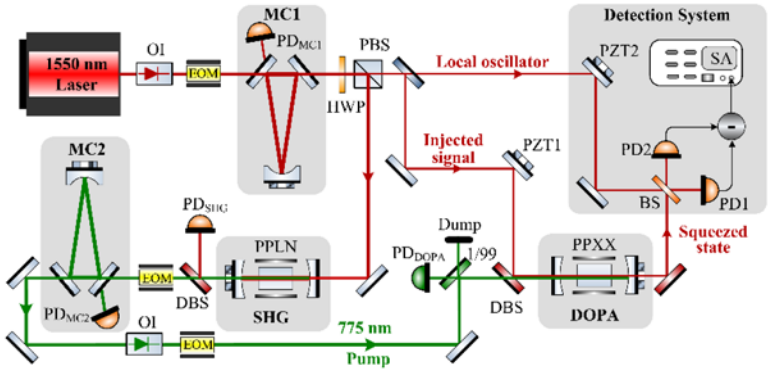

Fig. 3. Schematic of the experimental setup used to generate squeezed states from the DOPA using PPXX crystal. OI: optical isolator; EOM: electro-optic modulator; SHG: second harmonic generator; MC1: mode cleaner of 1550 nm; HWP: half-wave plate; PBS: polarizing beam splitter; MC2: mode cleaner of 775 nm; DBS: dichroic beam splitter; PZT1-2: piezo-electric transducer; DOPA: degenerate optical parametric amplifier; BS: 50/50 beam splitter; PD: photo detector; ⊖ : negative power combiner; SA: spectrum analyser.

The DOPA was composed of two concave mirrors with radii of 30 mm and a type-I phase matched PPKTP or PPLN crystal. The input coupler of the DOPA provided partial transmission (PT) at 775 nm ($T_{775\ nm}$ = 90.0%) and high reflection (HR) at 1550 nm ($R_{1550\ nm}$ > 99.8%). The output coupler provided PT at 1550 nm ($T_{1550\ nm}$ = 13%) and HR at 775 nm ($R_{775\ nm}$ > 99.7%). Both end faces of PPKTP and PPLN were antireflection coated for wavelengths of 1550 nm ($R_{1550\ nm}$ < 0.1%) and 775 nm ($R_{775\ nm}$ < 0.25%). The PPKTP crystal, with dimensions of 10 mm (length) × 2 mm (width) × 1 mm (thickness) and a poling period of 24.7 μm, and the PPLN crystal, with dimensions of 10 mm (length) × 10 mm (width) × 1 mm (thickness) and a poling period of 18.6 μm, were housed in a copper oven and temperature-controlled by a homemade temperature controller with an accuracy of 0.01 °C, separately. The temperature of PPKTP and PPLN were controlled at 34.5 °C and 135.2 °C to realize the optimum phase matching, respectively. The injected signal was also used to align the cavity and measure the classical gain of the DOPA.

When the relative phase between the pump and injected signal was locked to 0 using a piezo-electric transducer (PZT1), the DOPA was operated in a state of amplification. A bright phase quadrature squeezed state was produced from the DOPA. The squeezed field and LO were combined at a 50/50 beam splitter and detected by a pair of InGaAs photodiodes with the quantum efficiency of η = 92% (PD1 and PD2, HAMAMATSU Photonics K. K., G10899). The homodyne efficiency is defined by $\zeta = \eta_P \eta_V^2$. η_P is the propagation efficiency with a measured value of 98.5% and η_V is the homodyne visibility with a measured value of 99.7%. The photocurrents are amplified using two low-noise, high-gain amplifiers based on the bootstrapped trans-impedance amplifier technology and the combination of L-C (inductance and capacitance) [32]. A clearance of 16 dB between the shot noise and the electronic noise can be achieved at 5 MHz when the amplifier is illuminated by 6 mW laser. The common mode rejection ratio of two amplifiers is 35 dB. The relative phase between the squeezed field and LO was locked to 0 by using PZT2. The output photo-currents from the amplifiers were combined by the negative power combiner and recorded by a spectrum analyser (SA). The parameters of SA were set as: resolution bandwidth of 30 kHz, and video bandwidth of 300 Hz.

4. Discussion

To test the nonlinear performance of the PPXX crystal, a CW single-frequency laser at 1550 nm was single-passing the nonlinear crystal for frequency doubling. The SHG conversion efficiency as a function of the crystal temperature is shown in Fig. 4. The dots and solid

Optics EXPRESS

curves in Fig. 4 are experimental results and theoretical predictions according to the theory in [28], respectively. The measured maximum SHG conversion efficiency of PPLN is 4.08‰ at the optimum phase-matching temperature of 136 °C, as shown in Fig. 4(a). As a comparison, the measured maximum SHG conversion efficiency of PPKTP is 1.57‰ at the optimum phase-matching temperature of 35 °C, as shown in Fig. 4(b). It is apparent that the nonlinear conversion efficiency of PPLN is 2.6 times higher than that of PPKTP, but the optimum phase-matching temperature of PPKTP is low and close to the room temperature. Optical losses is a very important parameter for the efficient generation of squeezing, especially intra-cavity losses can devastate the squeezing level. To investigate the influence of the absorption of PPKTP and PPLN on the squeezing level, the absorption coefficients of PPKTP and PPLN at 1550 nm were measured using the thermal self-phase modulation technique [33], which is 1.35×10^{-4} cm^{-1} and 1.78×10^{-4} cm^{-1} for PPKTP and PPLN, respectively.

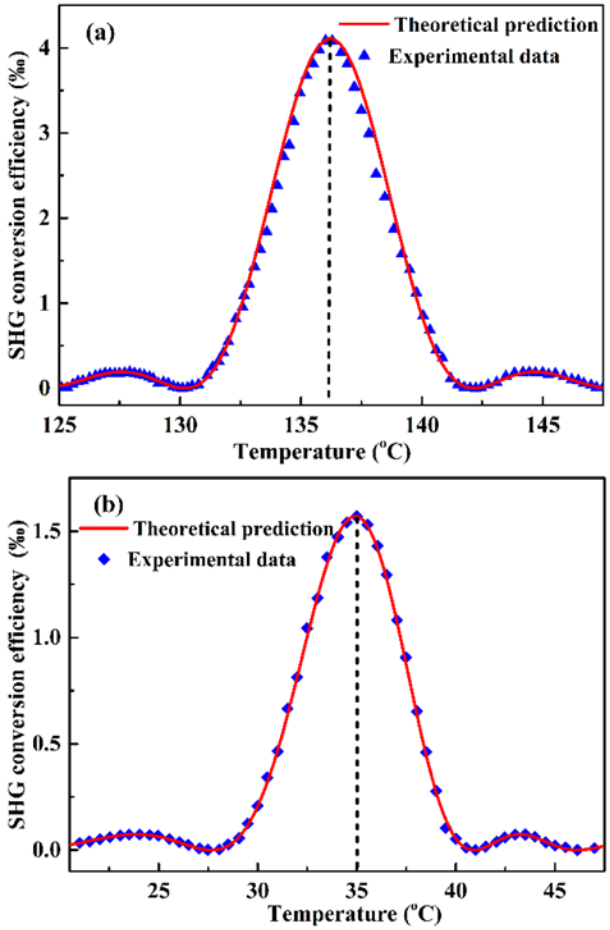

Fig. 4. SHG conversion efficiency as a function of the crystal temperature when a 1550 nm laser single-passes the PPLN crystal (a) and the PPKTP crystal (b). Dots are experimental data, solid curves are the theoretical predictions.

The measured threshold of the degenerate OPO (DOPO) using PPKTP and PPLN were 230 mW and 145 mW, respectively. The threshold of DOPO using PPLN is lower than using PPKTP due to larger nonlinear conversion efficiency of PPLN. When DOPA was subthreshold operated in the state of amplification, a bright phase quadrature squeezed state at 1550 nm was produced. The measured squeezing and anti-squeezing at analysis frequency of 5 MHz under different normalized pump power using PPKTP (blue circles) and PPLN (red

Optics EXPRESS

diamonds) are shown in Fig. 5(a) and 5(b), respectively. The SNL corresponds to the noise power of 6 mW LO power and a signal power that equal to the mean field power of the bright squeezed state, which was achieved by adjusting the power of the injected signal of the DOPA without the pump. A measured maximum squeezing of 6.8 dB of bright phase quadrature squeezed state with a mean field power of 120 μW was produced from the DOPA using PPKTP at a pump power of 160 mW and an injected signal power of 14 mW, and the corresponding anti-squeezing was 11.8 dB. It should be noted that the actual injected signal power in the DOPA cavity was about 20 μW because the injected signal was coupled into the cavity through the input coupler. By contrast, a measured maximum squeezing of 4.9 dB with a mean field output power of 45 μW was generated using PPLN at a pump power of 87 mW and an injected signal power of 9 mW, and the corresponding anti-squeezing was 10.7 dB.

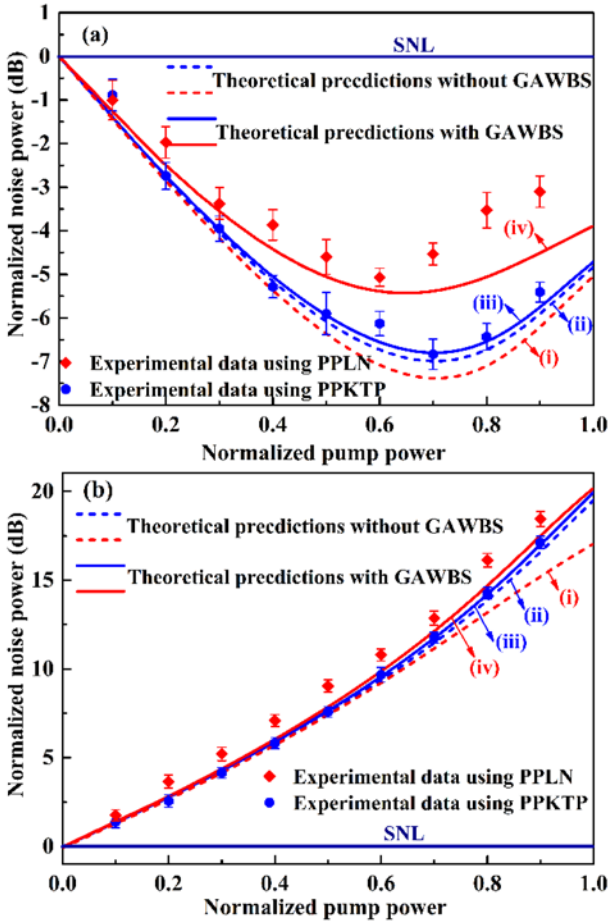

Fig. 5. Noise powers of output from DOPAs v.s. normalized pump power at analysis frequency of 5 MHz. (a) Squeezed noise. (b) Anti-squeezed noise. Blue circles and red diamonds are experimental data using PPKTP and PPLN, respectively. Dashed curves are theoretical predictions without considering GAWBS effect inside PPKTP (ii) and PPLN (i). Solid curves are theoretical predictions with considering GAWBS effect inside PPKTP (iii) and PPLN (iv).

Curves in Fig. 5 are the calculated normalized noise powers of output from DOPAs using Eq. (9) and the parameters of η = 0.92, ζ = 0.98, ξ = 0.85, and Ω = 5 MHz. Taking into account that the absorption coefficients of PPKTP and PPLN are different, γ is set as 0.500×10^8 s^{-1} and 0.501×10^8 s^{-1} for PPKTP and PPLN, respectively. Dashed curves represent the theoretical predictions without considering the effect of GAWBS inside PPKTP (curve ii) and

Optics EXPRESS

PPLN (curve i), respectively. It can be seen that a 7.4 dB squeezing can be obtained using PPLN at a normalized pump power of 0.7 if the effect of GAWBS inside PPLN is not considered, and the theoretical prediction has a large discrepancy with experimental results. Solid curves give the theoretical predictions considering the effect of GAWBS inside PPKTP (curve iii) and PPLN (curve iv), respectively. The theoretical prediction is in good agreement with experimental results when PPKTP is used. It can be see that the theoretical prediction has a discrepancy with experimental results when PPLN is used, the possible reason is that there is still other extra noise induced by thermal effects at a high temperature of nonlinear crystal and a high pump power. Clearly, the nonlinear conversion efficiency of PPKTP is lower than that of PPLN and the threshold of the DOPO using PPKTP is larger than using PPLN, but the large squeezing of phase quadrature squeezed state can be generated using PPKTP owing to low phase matching temperature and weak influence of the GAWBS effect in the crystal.

5. Conclusion

Bright phase quadrature squeezed states at 1550 nm were generated from DOPAs, which were subthreshold operated in the state of amplification, using PPLN and PPKTP, respectively. A measured squeezing of 6.8 dB with a mean field power of 120 μW was produced from the DOPA using PPKTP at a pump power of 160 mW. By contrast, a measured squeezing of 4.9 dB with a mean field output power of 45 μW was generated using PPLN at a pump power of 87 mW. Although the single-passing nonlinear conversion efficiency of PPLN is 2.6 times higher than that of PPKTP, and the measured threshold of the DOPO using PPLN is lower than using PPKTP, the measured phase quadrature squeezing using PPLN with the phase matching temperature of 135.2 °C is lower than that using PPKTP with the phase matching temperature of 34.5 °C. The degradation of squeezing of generated phase quadrature squeezed state using a nonlinear crystal with a high phase matching temperature is explained by a theoretical model of DOPAs including the extra phase noise caused by the effect of GAWBS within the nonlinear crystal. The PPKTP crystal is the best choice to prepare non-classical states of light that can be widely used in the application fields such as quantum information processing and high-precision quantum measurements.

Funding

National Key R&D Program of China (2016YFA0301401); Fund for Shanxi “1331 Project” Key Subjects Construction (1331KS).